Final Draft
of the original manuscript:

1 **Smart Metal-Polymer Bionanocomposites as Omnidirectional Plasmonic Black**

2 **Absorbers Formed by Nanofluid Filtration**

3 By *Mady Elbahri[*], Shahin Homaeigohar, Ramzy Abdelaziz, Tianhe Dai, Rania Khalil, Ahnaf Usman*

4 *Zillohu*

5 [*]Prof. M. Elbahri, Dr. Sh. Homaeigohar, Dr. T. Dai, A.U. Zillohu

6 Helmholtz-Zentrum Geesthacht, Institute of Polymer Research, Nanochemistry and Nanoengineering,

7 Max-Planck-Str.1, 21502, Geesthacht, Germany

8 E-mail: ((mady.elbahri@hzg.de))

9 Prof. M. Elbahri, R. Abdelaziz, Dr. R. Khalil

10 Faculty of Engineering, University of Kiel, Institute for Materials Science, Nanochemistry and

11 Nanoengineering, Kaiserstrasse 2,24143 Kiel, Germany

12 E-mail: ((me@tf.uni-kiel.de))

13 Dr. R. Khalil

14 Department of Physics, Faculty of Science, Zagazig University, Zagazig 44519, Egypt

15

16

18

19

1   **Here, we introduce the first smart plasmonic absorber based on metal-polymer**

2   **bionanocomposites performing via conformational changes of the biological functional agent i.e. a**

3   **protein. Such a progress was done through bridging the gaps between nanofluid filtration,**

4   **plasmonics and bioswitching. Initially, a biofunctionalized nanofibrous membrane was developed**

5   **that could filter out metal nanoparticles (<100 nm) from an aqueous stream with a high**

6   **separation efficiency (97%). This approach brings about a breakthrough in applicability of the**

7   **macroporous nanofibrous membranes for rejection of suspended nanosolids and extends the**

8   **application area beyond Microfiltration (MF) to Ultrafiltration (UF). This operative filtration in**

9   **next step leads to a novel synthesis route for plasmonic materials as formation of a smart free-**

10   **standing metal-polymer bionanocomposite able to act as an omnidirectional black absorber.**

11

12

13

14

15

16   **1. Introduction**

17   Bionanocomposites as a novel group of nanostructured hybrid materials possess a combination

18   of biopolymers and nanoscale inorganic solids.[1, 2] The biological component of the bionanohybrid not

19   only brings about a biocompatibility and environmentally friendly nature to the nanohybrid but also

20   stabilizes the inorganic solid.[3, 4] Moreover, the stimulus-responsive behaviour of the biological

21   component would provides the nanohybrid with a smart functionality.[5, 6]

22   As the second constituent, the inorganic nanocomponent e.g. metal nanoparticles show

23   promising properties in terms of optical, magnetic etc. [7] Exhibiting optimum structural and functional

1 properties arose from either the biological or inorganic moieties, these biohybrid materials have been

2 envisaged suitable for a diverse range of advanced applications such as plasmonics. [1, 6, 8]

3   Plasmonics is a rapidly growing field on the cutting edge of optical sciences, photonics and

4 nanotechnology. It aims to exploit the unique optical properties of metallic nanostructures to enable

5 routing and active manipulation of light at the nanoscale thereby creating fascinating optical devices

6 such as plasmonic absorbers. Nowadays, designing plasmonic black absorbers for a wide range of

7 applications e.g. photodectors [9-11], microbolometers [12] and thermophotovoltaic solar energy

8 convertors [13-17] is highly demanded.

9   Even though designing a plasmonic absorber at visible frequencies is still a challenge, among

10 the techniques used for this purpose; grating structured system, perforated metallic film and

11 metamaterial [18-20] could somewhat approach to such a desire. However, all the mentioned methods are

12 costly and suffer from the lack of flexibility and the absorbance obtained is limited to a narrow range of

13 frequencies. Advantageous over the previous techniques, recently we introduced a broadband plasmonic

14 absorber with almost 100% absorbance spanning the broad area of frequencies from UV to NIR. This

15 plasmonic absorber was made through sputter coating of a metal film with a metal/dielectric

16 nanocomposite. [21] As one step ahead to simplify the fabrication process and naturally to minimize the

17 costs, as the forthcoming study, we introduce devising a smart black absorber based on free-standing

18 nanocomposites in a fiber mat form.

19   While the fabrication of such nanocomposites is crucially limited by the strong tendency of

20 nanoparticles to aggregate on the polymeric surface.[22-25] Here, as a novel strategy, we developed an

21 operative fabrication method for plasmonic bionanohybrids based on a filtration process. To do so, a

22 membrane composed of electrospun nanofibers functionalized by a protein ligand is utilized. Separation

23 of metal nanoparticles from the respective aqueous suspension by this nanofibrous membrane would

1   give rise to formation of a bionanohybrid. Such a performance implies the applicability of the

2   membrane for water treatment by itself as well.

3   Electrospun nanofibrous membranes (ENMs) compared to their conventional counterparts are

4   more porous and possess an interconnected porous structure thereby show an extraordinary permeability

5   giving rise to a low energy consumption. Yet, such membranes suffer from low mechanical stability

6   also hydrophobicity and are usually as low selective as microfiltration (MF) membranes. As a

7   shortcoming for our fabrication approach, these membranes owing to their micro-sized pores are able to

8   capture only coarse suspended solids rather than nanosized substances e.g. metal nanoparticles. [26-31]

9   The promising solution to preserve the high permeability of the nanofibrous membranes while

10   optimizing their retention efficiency as prerequisites of an operative nanofluid filtration subsequently an

11   energy/cost efficient fabrication of a plasmonic nanohybrid is biofunctionalization of the nanofibers.

12   Our filtration based fabrication method of the bionanocomposite is assumed to benefit the

13   unique smart conformational and structural properties of the biofunctional agent with a novel dual role

14   as: 1) the capturer of metallic nanoparticles also 2) the structural tuner of the first smart omnidirectional

15   broadband black absorber with almost 100% absorbance spanning the visible frequencies.

16   To the best of our knowledge, filtration using macroporous electrospun nanofibrous mats to

17   capture nanoparticles and adopting this approach as a facile route to fabricate a tunable nanocomposite

18   black absorber has never been reported. Indeed, through this study we bridge the gap between several

19   fields including filtration, plasmonics and bioswitching.

20

21   **2. Results and Discussions**

22   As the current study, we functionalized poly(acrylonitrile-co-glycidyl methacrylate)

23   (PANGMA) nanofibers through surface immobilization with Bovine Serum Albumin (BSA). BSA

24   acting as the capturer component is a cheap serum albumin protein, widely used in numerous

1　biochemical applications. Moreover, PANGMA as a new polymeric material is a copolymer of

2　acrylonitrile (AN) and glycidyl methacrylate (GMA).[32] This polymer possesses a suitable chemical

3　stability induced by the strong backbone of polyacrylonitrile. Moreover, the presence of a free and

4　active epoxy group on GMA could lead to a high functionality thereby the feasibility of a variety of

5　activation/coupling chemistries for the covalent binding of capturers. In the current study, the

6　nanofibers are functionalized based on the extremely simple and conventional epoxy-amino reaction

7　between the amine groups on BSA and epoxy groups on PANGMA. [32, 33]

8　　　　Functionalization mechanism of PANGMA is based on ring opening of the epoxide groups of its

9　GMA part when attacked by amine containing BSA. The result of such a reaction is formation of the

10　secondary amine and hydroxyl groups. Such an assumption is proved by the surface chemical analysis

11　results shown in **Figure 1a**. Successful reaction between primary amine groups of BSA and epoxides of

12　PANGMA is emphasized by vanishing the characteristic peak of epoxy group appearing at 908 cm^{-1} for

13　the neat nanofibers. In addition, the peaks emerging at 1650 cm^{-1} and 1530 cm^{-1} are the vibration peaks

14　of amide I and amide II groups in BSA molecules. The peaks at 3300 and 3600 cm^{-1} are related to the

15　secondary amine and hydroxyl groups, respectively, generated during the opening of the epoxy group

16　by the primary amine groups of BSA. [34, 35]

17　　　　Possessing lots of primary amine groups, BSA can also react with two adjacent PANGMA

18　nanofibers leading to a cross linked structure. While, the overview pictures obtained by scanning

19　electron microscopy (SEM) (**Figures 1bI,II**) reveal no significant difference in term of porosity

20　between the neat and functionalized nanofibrous mats, the cross sectional image of the latter group

21　(**Figure 1bIII**) clearly indicates that the submicrometer fibers are interconnected by nanometer protein

22　wires. This behaviour was not observed for the neat membrane. Such an increase of the netting points of

23　the web and interfiber bondings are expected to strengthen the membrane. [36, 37] This effect is

24　intensified by crosslinking of the PANGMA molecules inside the nanofibers while functionalization.

1   Indeed, the biofunctionalization giving rise to inter/intrafiber bondings leads to a significantly higher

2   mechanical stability in terms of elastic modulus (E) and tensile strength (σ) as 194% and 300% increase,

3   respectively, compared to those of the neat PANGMA ENM. A mechanically strong nanofibrous

4   membrane can resist against pore collapse while filtration subsequently possesses a longer life span and

5   lower energy consumption.[38] A water filtration test under a 1 bar pressure, readily showed that the

6   mechanically stronger BSA/PANGMA ENM is much more permeable ($\sim$ 45 kl.h^{-1}.m^{-2}) than its neat

7   counterpart. Yet, some part of this higher permeability is attributed to the superhydrophilicity of the

8   functionalized membranes arose from emergence of the secondary functional groups which could lower

9   the filtration resistance. As proved via a water contact angle measurement, while the neat membrane

10   showed a water contact angle of 130°, this value for the biofunctionalized one was only 5° implying

11   their hydrophobicity and superhydrophilicity, respectively.

12   Applicability of electrospun nanofibrous membranes is significantly promoted when they are

13   able to perform beyond a MF membrane capturing not only coarse suspended solids but also nanosolids

14   much smaller than the pore size. Here, we aim to show that functionalization through BSA

15   immobilization, brings about a highly selective energy saving UF ENM able to capture metal

16   nanoparticles. As a proof of the concept, gold (Au) nanoparticles containing aqueous suspensions were

17   filtered. The nanoparticles used in the model feed system had a size of 20, 40 and 80 nm in the range of

18   UF.

19   Retention ability of the BSA/PANGMA ENMs for the gold nanoparticles is demonstrated in

20   **Figure 1c**. As the control experiment to compare the filtration performance of the functionalized

21   PANGMA ENM with its neat counterpart, the suspension containing 40 nm Au nanoparticles was

22   randomly selected. While the neat PANGMA ENM is able to reject a negligible part (1.5 %) of the 40

23   nm Au nanoparticles, the biofunctionalized ENM rejects 72.5% of the nanoparticles of the same size.

24   Visual inspection of the feed and permeate samples clearly reveals the high retention ability of the

1 BSA/PANGMA ENM compared to its neat counterpart. As seen in **Figure 1d**, color intensity of the

2 feed sample drastically decreases after permeation through the biofunctionalized ENM.

3 The retention efficiency for 80 nm Au nanoparticles is even more as high as 97 %, whereas this

4 value for the 20 nm nanoparticles reduces to 70%, still high and promising. In addition to such an

5 extraordinary retention efficiency, the permeate flux recorded when filtration of 80 nm Au suspension,

6 was also considerable as high as 9000 $l.h^{-1}.m^{-2}$ much higher than that reported for conventional

7 micro/ultrafiltration membranes. [27] Noteworthy, there was no major feed pressure while filtration and

8 the experiment was performed under the atmospheric pressure implying a very low energy

9 consumption.

10 As shown in **Figures 2 a-c**, the reason for such a high retention efficiency by the

11 BSA/PANGMA ENMs should be sought in the conformational change of the immobilized BSA.

12 Indeed, the configuration of BSA as folded or unfolded would play a governing role in its capturing

13 ability of nanoparticles. In the folded state i.e. "α- helix", the tryptophan and cysteine residue groups

14 which are able to interact with metal nanoparticles are mostly located within the protein structure and

15 not exposed.[39] Furthermore, owing to the strong internal hydrogen bonds between the peptide groups,

16 other functional groups such as amine based groups are less available on the surface as well. However, a

17 conformational change during the filtration stimulates the unfolding of BSA as β- turn, thereby

18 emergence of these active groups on the surface capable ideally to capture the nanopartciles.

19 This alteration is traceable through ATR-FTIR measurements (**Figure 2a**) as replacement of the

20 bands assigned to α- helix secondary structure of BSA (1650–1658 cm^{-1}) predominated in dry state with

21 those of turns (1666-1673 cm^{-1})[40, 41] in wet state. As a result, previously buried peptide bonds such as

22 those appeared in wet state at 1210 and 1721 cm^{-1} (corresponding to C- N and C=O) and amino acid

23 side chains are exposed and can interact with the aqueous environment. Such a transformation leads to

24 binding considerably more water [42] giving rise to a swollen structure. From one hand, expansion of the

1   protein on the surface of the nanofibers makes a smaller pore size and more steric hindrance by growing

2   nanofibers (**Figures 2b,c**). On the other hand, upon conformational change the functional protein groups

3   become exposed on the surface. These binding groups could capture the nanoparticles and stabilize

4   them by strong protein- metal nanoparticle interactions such as ionic interaction, hydrogen bonding,

5   Van der Waals and hydrophilic interactions [43-45], thus Au nanoparticles stick to BSA protein.

6   Combination of these effects reminds us the hunting behaviour of a carnivorous plant and results in a

7   significantly high retention efficiency for the membrane being studied. This retention ability is

8   intensified as soon as adsorption of the first batch of metal nanoparticles to the functionalized

9   nanofibers leading to gradual change of the surface color as well. Interestingly, as long as the filtration

10   goes on i.e. after the 2nd to 3rd cycle, more nanoparticles are adsorbed onto the nanofibers thereby the

11   surface color becomes darker and finally shifts to black.

12   Biofunctionalization not only could revolutionize filtration performance of an ENM but also it

13   can equip the membrane to some further abilities e.g. creating plasmonic nanocomposites. For instance,

14   the Au nanoparticle/BSA/PANGMA nanofibrous membrane as dried possesses a reddish color

15   attributed to the gold nanoparticles adsorbed on the membrane's surface. The intensity of the color

16   strongly depends on the amount of the nanoparticles adsorbed and indirectly on the filtration duration.

17   However, when the membrane is soaked in water to remove the weakly adsorbed i.e. "non-captured"

18   nanoparticles, the membrane's color becomes black. Drying the membrane again leads to returning the

19   red color. We repeated this process for ten cycles with a fully repeatability. Such a performance certifies

20   the applicability of our smart bionanocomposite in development of switchable plasmonic materials.

21   The influence of the water-induced structural changes on the collective optical properties of the

22   nanocomposites is shown in **Figure 3a**. As observed in this figure, there is a tunable coloration of the

23   sample from red to black in dry and wet states, respectively. UV-vis measurements support the naked

24   eyes observation. **Figure 3b** shows the reflection spectra of the nanocomposite in dry and wet states at

1   the start and after 10 cycles of repetitions. Obviously, depending on the hydration states, the color of the

2   membrane changes from red, recognized by a reflection dip at 537 nm, to black with vanishing

3   reflections in the visible ranges. More specifically, the reflection measurement of the black absorber

4   shows wide resonances broadly spanning the spectral range from NUV to NIR with an alleviated

5   reflection and a complete absorption of nearly 100%.

6   **Figure 3c** clearly confirms that the adsorption of tiny gold nanoparticles onto the functionalized

7   nanofibers gives rise to development of the red plasmonic nanocomposites. The black state is associated

8   with the tunable conformation which was investigated by Cryo-SEM. As seen in **Figure 3d**, the black

9   hybrid could be resembled to a swollen open porous nanostructured foam. Formation of the porous

10   structure reveals a phase separation in the fully hydrated membrane. Indeed the fabricated

11   bionanocomposite is characterized by the presence of hydrophilic domains embedded in / attached on

12   the hydrophobic polymer matrix. The hydrophobic domains apply considerable constraints upon the

13   hydrophilic amorphous regions, restricting their swelling by inhibiting deformation parallel to their

14   surfaces. Owing to the limited segmental mobility, an osmotic pressure is developed in the matrix which

15   can lead to the formation of voids. Expansion of the voids is opposed by the vitrification of the

16   polymer-rich matrix surrounding them. Thus, the balance between the two opposite forces gives rise to

17   the formation of porous structures decorated by the nanoparticles in a nanoaggregation- like fashion.

18   Because of the nanoaggregation, there is a diversity of structures which reinforce the localized

19   plasmon excitations and strongly couple them in a broad spectral range. [46-50] It is well known that in

20   the case of closely spaced nanoparticles (near percolation), strong near field coupling occurs and energy

21   can be efficiently trapped. [51] The light trapping is intensified when the incident light is diffracted or

22   scattered by the accumulated nanoparticles. Hereby, the light is encouraged to enter into the structure

23   rather than to reflect back. Utilization of a layer thick enough to prevent the light from passing through

1 and able to trap the energy thereby to suppress the reflection, will obstruct the incident light and make

2 the device as a black absorber.

3 However, it is not yet clear if our porous metal-polymer nanocomposite possessing the pores as

4 large as the wavelength of the incident radiation in visible frequency, could behave as an

5 "electromagnetic black body".

6 The theoretical work by Narimanov and Kildishev [52] on an optical metamaterials based

7 omnidirectional light absorber shows that all the optical waves hitting the concentrator [53] are trapped

8 and absorbed. The proposed hybrid device is composed of non-resonant and resonant metamaterial

9 structures (spirally or a cylinder), which can trap and absorb electromagnetic waves coming from all

10 directions without any reflections due to the local control of electromagnetic fields. Similarly, our metal

11 polymer bionanocomposite black absorber is not sensitive to the incidence angle of the light. **Figure 3e**,

12 illustrates that there is no considerable angular dependence of the reflection measurement of the sample

13 ranging from 30° to 60° on corresponding reflectivity of the structure in all the incidence angels.

14 However, our finding needs further experiments currently being in progress in our laboratory. On the

15 whole, to the best of our knowledge our work is the first report on design of a black plasmonic absorber

16 at the visible frequency using free-standing nanocomposites via a nanofluid filtration process.

17 Noteworthy, besides creation of the black absorber, the membrane could be used for a novel water

18 treatment i.e. separation of metal nanoparticles from waste water streams as well. For example, silver

19 nanoparticles are frequently used in consumer products (e.g. in socks to inhibit odor-causing bacteria)

20 due to their promising potential of bactericidal. However, recent studies have shown that such

21 nanoparticles in case release can kill also benign bacteria being used in removal of ammonia from

22 wastewater treatment systems.[54] Hence, there is a necessity in removal of metal nanoparticles released

23 in waste water streams. As proved through the current study, our novel membrane showed such a

24 potential.

1

2   **3. Conclusion**

3   In summary, by developing a novel bio assisted nanofluid filtration route, a smart perfect

4   plasmonic black absorber based on a metal-polymer bionanocomposite is designed and introduced for

5   the first time. Such a progress was done through bridging the gaps between nanofluid filtration,

6   plasmonics and bioswitching. Initially, a biofunctionalized nanofibrous membrane was developed that

7   could filter out metal nanoparticles (<100 nm) from an aqueous stream with a high separation efficiency

8   (97%), an optimum permeability, mechanical stability also wettability. This approach brings about a

9   breakthrough in applicability of the macroporous nanofibrous membranes for rejection of suspended

10   nanosolids and extends the application area beyond MF to UF. This operative filtration in next step

11   leads to a novel synthesis route for plasmonic materials as formation of a smart free-standing metal-

12   polymer bionanocomposite able to act as a black absorber.

13

14   **4. Experimental**

15   *Materials:* Poly(acrylonitrile-co-glycidyl methacrylate) (PANGMA) was synthesized by

16   Helmholtz-Zentrum Geesthacht (HZG) (previously GKSS Forschungszentrum GmbH)[55] with a

17   molecular weight (M_n) of ca. 100,000 g.mol^{-1} and GMA content of 13 mol%. Bovine Serum Albumin

18   (BSA) (dried powder) and Phosphate Buffered Saline (PBS) were purchased from Sigma-Aldrich Co.

19   *N,N*-dimethylformamide (DMF) and methanol were purchased from Merck KGaA. All the chemicals

20   were directly used without purification.

21   While, the Au nanoparticles of 20 nm (Gold colloid G1652, G1402) were purchased from

22   Sigma-Aldrich Co. and used without further purification, those of 40 and 80 nm were made using

23   sodium citrate reduction method reported by Wang.[56]

1   *Preparation of PANGMA ENMs by electrospinning:* Briefly, prepared PANGMA solution (20

2   wt%) in *N,N*-dimethylformamide (DMF) was fed with a constant rate of 1.1 ml.h^{-1} into a needle by

3   using a syringe pump (Harvard Apparatus, USA). By applying a voltage of 15-20 kV (Heinzinger

4   Electronic GmbH, Germany) electrospinning was done on an Aluminum (Al) foil located 25 cm above

5   the needle tip for 4 h. After all, the nanofibrous mat was peeled off from Al foil and dried under vacuum

6   at 30 °C for 24 h to remove the residual solvent.

7   *BSA immobilization:* PANGMA ENMs were immersed into the BSA/PBS buffer (5 mg.ml^{-1})

8   (pH 6.8) and the mixture was moderately shaken at 55 °C for 24 h. Then, the membranes were taken out

9   and washed several times by PBS buffer (pH 6.8) to remove all the unbound BSA. Finally, the BSA

10   immobilized PANGMA ENMs were carefully washed with deionized water and dried under vacuum at

11   30 °C for 24 h.

12   *Morphological and structural characterizations:* The morphology of the PANGMA ENMs was

13   observed with a scanning electron microscope (LEO Gemini 1550 VP, Zeiss). The wet sample was

14   investigated by a Scanning Electron Microscope Hitachi S 4800 equipped with Gatan Alto 2500 Cryo

15   Preparation System.

16   Optical measurements of the dry and wet composite samples were done using a UV-Vis/IR

17   spectrometer (Lambda 900).

18   Chemical surface analysis of both the neat and BSA immobilized PANGMA ENMs was

19   performed by Fourier Transform Infra Red Spectrometry (FTIR). Attenuated total reflection Fourier

20   transform infrared (ATR-FTIR) spectra were recorded using a Bruker Equinox 55 spectrometer.

21   *Mechanical characterization (tensile test):* The tensile mechanical properties of the PANGMA

22   ENMs were characterized by a tensile machine (Zwick/Roell Z020-20KN, Germany) equipped with a

23   20-N load-cell at ambient temperature. The cross-head speed was 2 mm.min^{-1} and the gauge length was

1 20 mm. The reported tensile moduli, tensile strengths and elongations represented average results of 10

2 tests.

3   *Wettability characterization:* Wettability of the PANGMA ENMs was characterized through

4 water contact angle measurement, using a contact angle analysis system (Kruess DSA 100, Germany).

5 A 5 µl droplet was dispensed on the membrane and the resultant angle was measured.

6   *Water permeability analysis:* Water Permeability of the PANGMA ENMs as neat and

7 functionalized was evaluated through a water flux measurement using a custom-built set-up (shown in

8 [57]). The circular membranes (d=20 mm) were stamped out and placed over a poly(*p*-phenylene sulfide)

9 (PPS) technical nonwoven support layer. 300 ml water was passed through the membranes under a 1 bar

10 applied pressure. The water flux was calculated by Equation (1):

11 $$J = \frac{Q}{A.\Delta t}$$ (1)

12   where J is the water flux (l.h^{-1}.m^{-2}), Q is the permeated volume of water (l), A is the effective

13 area of the ENMs (m^2), and Δt is the sampling time (h). All the flux measurements were repeated three

14 times.

15   *Retention test with metal nanoparticle containing aqueous suspension:* The retention capability

16 of the neat and biofunctionalized PANGMA ENMs was determined using aqueous suspensions

17 containing gold nanoparticles with different average particle sizes including 20, 40 and 80 nm. The

18 suspensions (20 ml) were passed through the membranes with the same configuration as those in the

19 water permeability test. This process was done as three successive cycles i.e. the first permeate was

20 used as the second feed and the second permeate as the third feed. Meanwhile, the permeation time was

21 recorded. Noteworthy, the filtration was performed under a negligible hydrostatical pressure i.e. no

22 considerable feed pressure.

23   Already assessing gold nanoparticle aqueous suspension calibration curve, the concentrations of

24 gold nanoparticles in the original feed and permeate were determined by UV-Vis spectroscopy

1 (HITACHI U-3000, HITACHI). The retention efficiency (RE) was determined according to Equation

2 (2):

3
$$RE = (1 - \frac{C_{permeate}}{C_{feed}}) \times 100\% \qquad\qquad (2)$$

4 where C_{permeate} and C_{feed} are the permeate and feed concentrations, respectively.

5

6

7 **Acknowledgement**

13 Received: ((will be filled in by the editorial staff))

14 Revised: ((will be filled in by the editorial staff))

15 Published online: ((will be filled in by the editorial staff))

16

17 **References:**

18 [1] M. Darder, P. Aranda, E. Ruiz-Hitzky, *Adv. Mater.* **2007**, *19*, 1309.

19 [2] E. R. Ruiz-Hitzky, M. Darder, P. Aranda, *J.Mater. Chem.* **2005**, *15*, 3650.

20 [3] C. Mao, D. J. Solis, B. D. Reiss, S. T. Kottmann, R. Y. Sweeney, A. Hayhurst, G. Georgiou, B.

21 Iverson, A. M. Belcher, *Science* **2004**, *303*, 213.

22 [4] R. Brayner, M. J. Vaulay, F. Fievet, T. Coradin, *Chem. Mater.* **2007**, *19*, 1190.

[5]   D. Roy, J. N. Cambre, B. S. Sumerlin, *Prog. Polym. Sci.* **2010**, *35*, 278.

[6]   C. Aime, I. B. Rietveld, T. Coradin, *Chem. Phys. Lett.* **2011**, *505*, 37.

[7]   F. Faupel, V. Zaporojtchenko, T. Strunskus, M. Elbahri, *Adv. Eng. Mater.* **2010**, *12*, 1177.

[8]   M. Alsawafta, S. Badilescu, V.-V. Truong, M. Packirisamy, *Nanotechnology* **2012**, *23*, 065305.

[9]   Y. Ahn, J. Dunning, J. Park, *Nano Lett.* **2005**, *5*, 1367.

[10]   Y. Gu, E. S. Kwak, J. L. Lensch, J. E. Allen, T. W. Odom, L. J. Lauhon, *Appl. Phys. Lett.* **2005**, *87*, 043111.

[11]   O. Hayden, R. Agarwal, C. M. Lieber, *Nat. Mater.* **2006**, *5*, 352.

[12]   P. L. Richards, *J.Appl. Phys.* **1994**, *76*, 1.

[13]   T. J. Coutts, *Renew. Sustain. Energy Rev.* **1999**, *3*, 77.

[14]   S. Y. Lin, J. Moreno, J. G. Fleming, *Appl. Phys. Lett.* **2003**, *83*, 380.

[15]   H. Sai, H. Yugami, *Appl. Phys. Lett.* **2004**, *85*, 3399.

[16]   M. Law, L. E. Greene, J. C. Johnson, R. Saykally, P. Yang, *Nat. Mater.* **2005**, *4*, 455.

[17]   B. Tian, X. L. Zheng, T. J. Kempa, Y. Fang, N. F. Yu, G. H. Yu, J. L. Huang, C. M. Lieber, *Nature (London)* **2007**, *449*, 885.

[18]   V. G. Kravets, F. Schedin, A. N. Grigorenko, *Phys. Rev. B* **2008**, *78*.

[19]   H. Tao, C. M. Bingham, A. C. Strikwerda, D. Pilon, D. Shrekenhamer, N. I. Landy, K. Fan, X. Zhang, W. J. Padilla, R. D. Averitt, *Phys. Rev. B* **2008**, *78*.

[20]   N. Liu, M. Mesch, T. Weiss, M. Hentschel, H. Giessen, *Nano Lett.* **2010**, *10*, 2342.

[21]   M. K. Hedayati, M. Javaherirahim, B. Mozooni, R. Abdelaziz, A. Tavassolizadeh, V. S. K. Chakravadhanula, V. Zaporojtchenko, T. Strunkus, F. Faupel, M. Elbahri, *Adv. Mater.* **2011**, *23*, 5410.

[22]   Y. Wang, Q. Yang, G. Shan, C. Wang, J. Du, S. Wang, Y. Li, X. Chen, X. Jing, Y. Wei, *Mater. Lett.* **2005**, *59*, 3046.

[23]   H. K. Lee, E. H. Jeong, C. K. Baek, J. H. Youk, *Mater. Lett.* **2005**, *59*, 2977.

1 [24] I. Hayakawa, Y. Iwamoto, K. Kikuta, S. Hirano, *Sens. Actuators B* **2000**, *62*, 55.

2 [25] Z. Zhang, M. Han, *J.Mater. Chem.* **2003**, *13*, 641.

3 [26] V. Thavasi, G. Singh, S. Ramakrishna, *Energy Environ. Sci.* **2008**, *1*, 205.

4 [27] S. Ramakrishna, R. Jose, P. S. Archana, A. S. Nair, R. Balamurugan, J. Venugopal, W. E. Teo,

5 *J. Mater. Sci.* **2010**, *45*, 6283.

6 [28] SSh Homaeigohar, K Buhr, K. Ebert, *J. Mem. Sci.* **2010**, *365*, 68.

7 [29] D. Aussawasathien, C. Teerawattananon, A. Vongachariya, *J. Membr. Sci.* **2008**, *315*, 11.

8 [30] R. Gopal, S. Kaur, Z. W. Ma, C. Chan, S. Ramakrishna, T. Matsuura, *J. Membr. Sci.* **2006**, *281*,

9 581.

10 [31] R. Gopal, S. Kaur, C. Y. Feng, C. Chan, S. Ramakrishna, S. Tabe, T. Matsuura, *J. Membr. Sci.*

11 **2007**, *289*, 210.

12 [32] T. Godjevargova, V. Konsulov, A. Dimov, *J. Membr. Sci.* **1999**, *152*, 235.

13 [33] T. Dai, N. Miletic, K. Loos, M. Elbahri, V. Abetz, *Macromol. Chem. Phys.***2010**, *212*, 319.

14 [34] M. Gonzalez, P. Kadlec, P. Spepanek, A. Strachota, L. Matejka, *Polymer* **2004**, *45*, 5533.

15 [35] J. Gonzalez-Benito, *J. Colloid Interface Sci.* **2003**, *267*, 326.

16 [36] A. Romo-Uribe, L. Arizmendi, M. E. Romero-Guzman, S. Sepulveda-Guzman, R. Cruz-Silvan,

17 *ACS Appl. Mater. Interfaces* **2009**, *1*, 2502.

18 [37] S. Bal, *Mater. Des.* **2010**, *31*, 2406.

19 [38] SSh Homaeigohar, M. Elbahri, *J. Colloid Interface Sci.* **2012**, *372*, 6.

20 [39] D. Zhang, O. Neumann, H. Wang, V. M. Yuwono, A. Barhoumi, M. Perham, J. D. Hartgerink,

21 P. Wittung-Stafshede, N. J. Halas, *Nano Lett.* **2009**, *9*, 666.

22 [40] E. G. Ferrer, A. Bosch, O. Yantorno, E. J. Baran, *Bioorg. Med. Chem.* **2008**, *16*, 3878.

23 [41] H. El-Sherif, M. El-Masry, M. F. Abou Taleb, *J. Appl. Polym. Sci.* **2009**, *115*, 2050.

24 [42] D. H. Chou, C. V. Morr, *J. Am. Oil Chem. Soc.* **1979**, *56*, A53.

1   [43]   I. Lynch, K. A. Dawson, *Nano Today* **2008**, *3*, 40.

2   [44]   T Cedervall, I Lynch, S Lindman, T Berggard, E Thulin, H Nilsson, KA Dawson, S. Linse,

3   *PNAS* **2007**, *104*, 2050.

4   [45]   X. L. Kong, L. C. L. Huang, C. M. Hsu, W. H. Chen, C. C. Han, H. C. Chang, *Anal. Chem.*

5   **2005**, *77*, 259.

6   [46]   F. Brouers, D. Rauw, J. P. Clerc, G. Giraud, *Phys. Rev. B* **1994**, *49*, 14582.

7   [47]   G. A. Niklasson, *J. Appl. Phys.* **1987**, *62*, 258.

8   [48]   V. A. Markel, L. S. Muratov, M. I. Stockman, T. F. George, *Phys. Rev. B* **1991**, *43*, 8183.

9   [49]   V. M. Shalaev, R. Botet, *Phys. Rev. B* **1994**, *50*, 12987.

10   [50]   M. I. Stockman, L. N. Pandey, L. S. Muratov, T. F. George, *Phys. Rev. B* **1995**, *51*, 185.

11   [51]   V. Shalaev, Ed. *Optical properties of nanostructured random media*, Springer-Verlag Berlin,

12   Heidelberg **2002**.

13   [52]   E. E. Narimanov, A. V. Kildishev, *Appl. Phys. Lett.* **2009**, *95*.

14   [53]   A. V. Kildishev, L. J. Prokopeva, E. E. Narimanov, *Optics Express.* **2010**, *18*, 16646.

15   [54]   Science News, in *ScienceDaily*, **Apr. 29, 2008**.

16   [55]   H. G. Hicke, I. Lehmann, G. Malsch, M. Ulbricht, M. Becker, *J. Membr. Sci.* **2002**, *198*, 187.

17   [56]   F. Wang, *J. Foreign Med* **1991**, *12*, 145.

18   [57]   SSh Homaeigohar, H Mahdavi, M. Elbahri, *J. Colloid Interface Sci.* **2012**, *366*, 51.

19

1
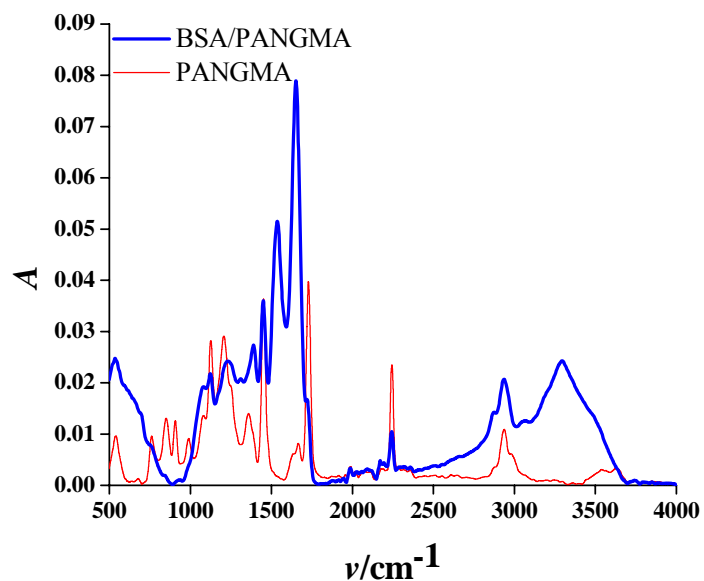
2   **Figure 1a** ((ATR-FTIR spectra of the PANGMA ENMs before and after BSA immobilization(A

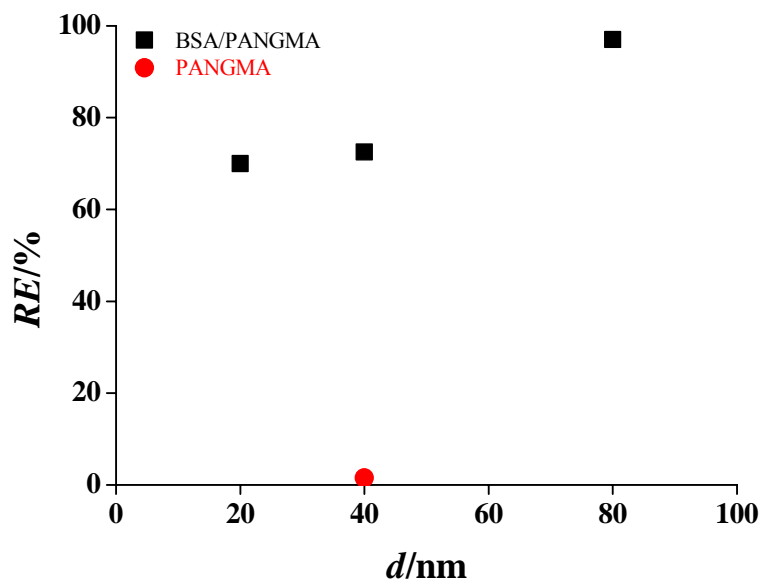3   and v represent absorbance and wavenumber, respectively)))
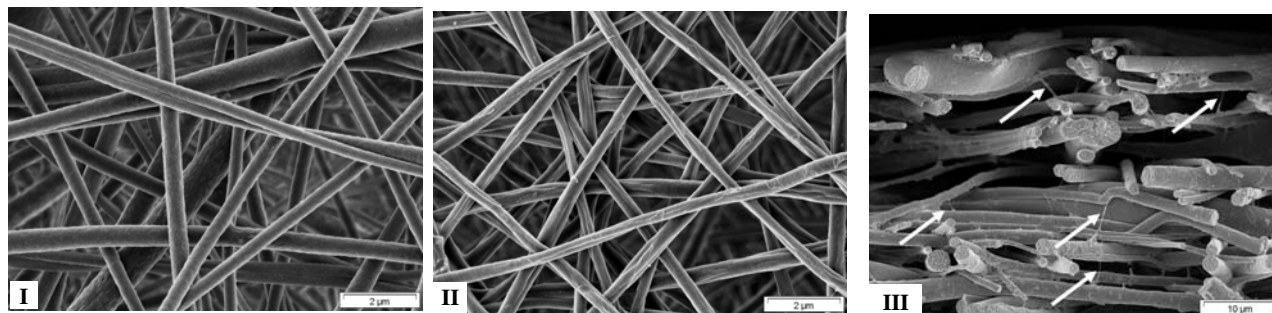

4   **Figure 1b** ((SEM micrographs of the PANGMA nanofibers as neat (I: overview) and BSA

5   immobilized (II: overview and III: cross-section; arrows indicate the BSA induced cross linking of the

6   nanofibers)))

1

2   **Figure 1c** ((Extraordinary nanofluid filterability after biofunctionalization proved via UV-vis

3   measurements(d at the x-axis represents the nanoparticle diameter)))
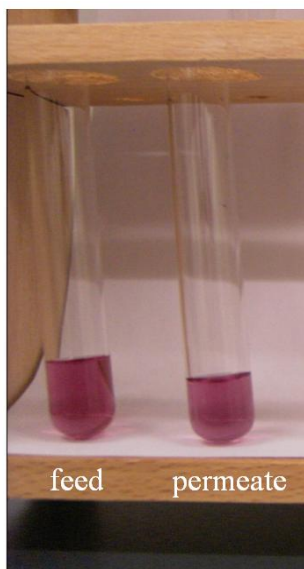
(I)   (II)

4

5   **Figure 1d** ((Extraordinary nanofluid filterability after biofunctionalization proved via visual

6   comparisons between the feed and permeated samples through the neat (I) and BSA/PANGMA ENMs

7   (II)))

1
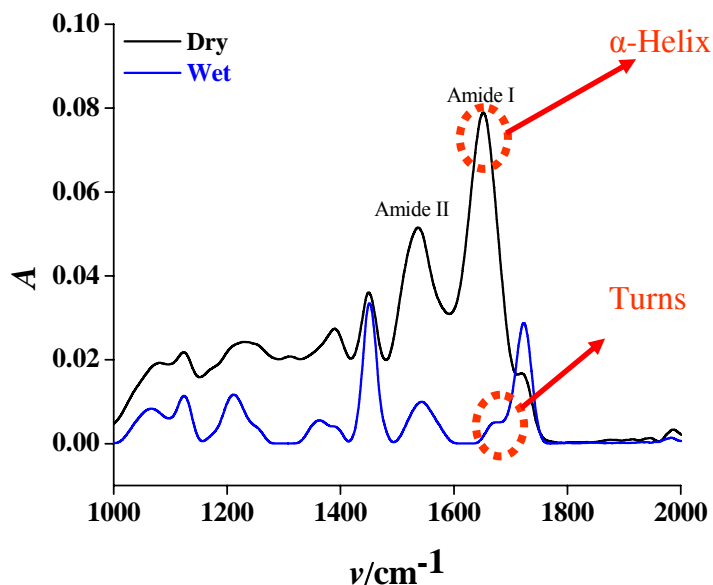
2   **Figure 2a** ((ATR-FTIR spectra of the BSA/PANGMA ENMs as dry (the black upper line) and

3   wet (the blue lower line)))

4
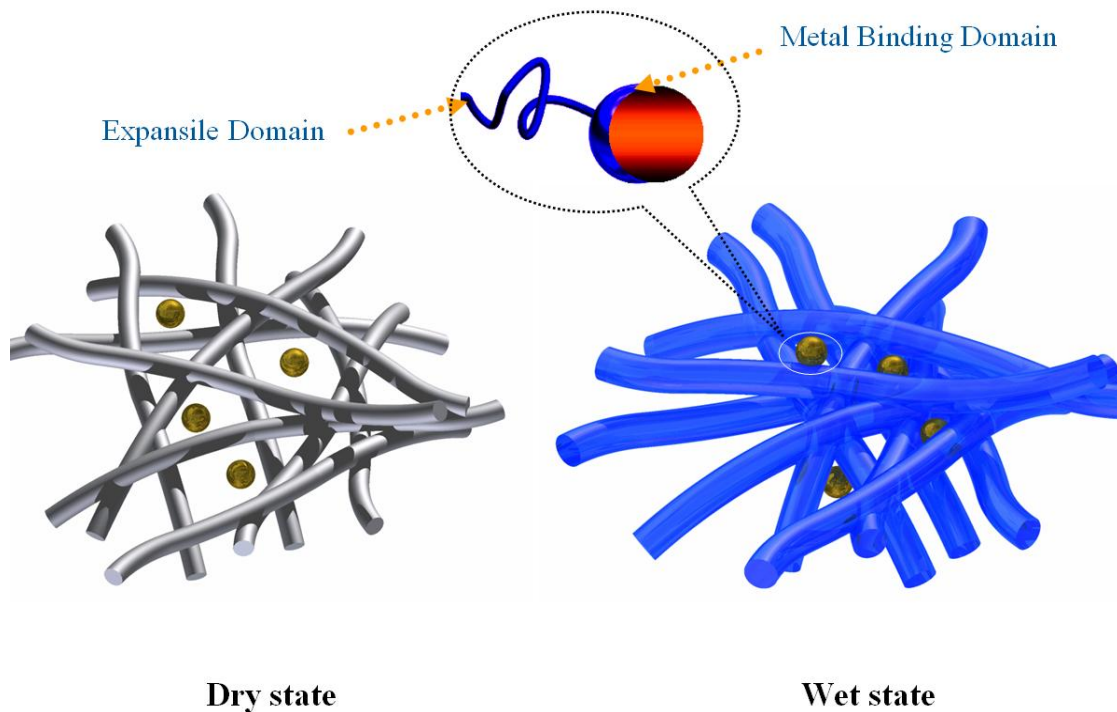
5   **Figure 2b** ((The sketch illustrates how the swollen functionalized nanofibers capture the

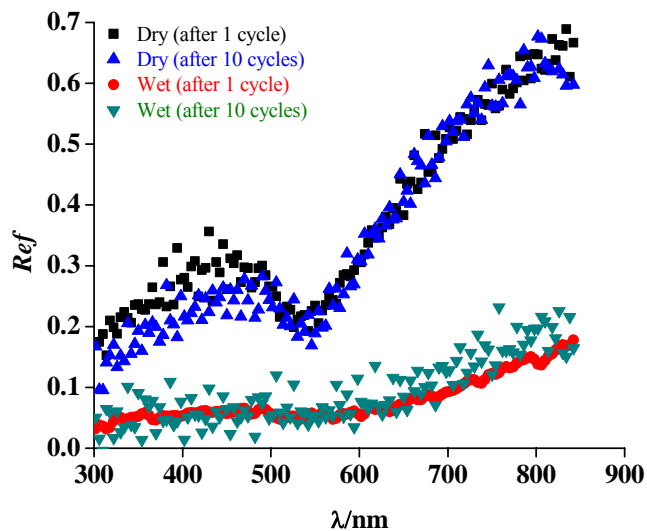6   nanoparticles))
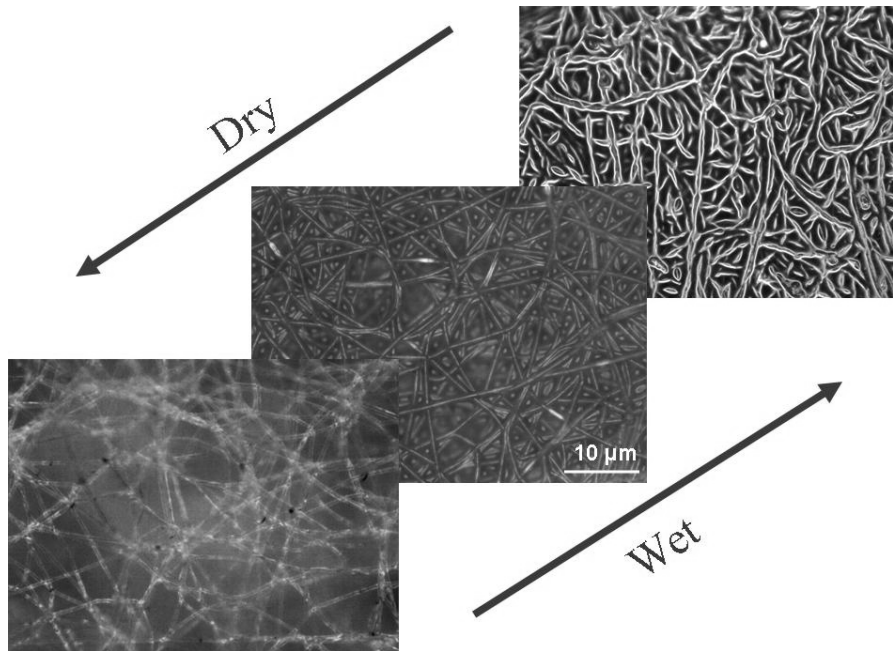
1

2

3

4   **Figure 2c** ((The optical images show morphological change of the membrane and the reversible

5   swelling of the functionalized nanofibers in wet and dry states implying a smart performing membrane))

6
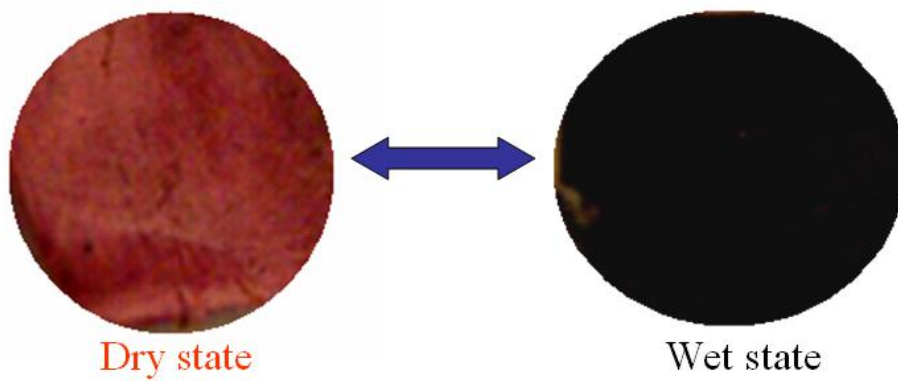
7   **Figure 3a** ((Tunable coloration of the surface of the membrane at dry (red) and wet (black)

8   states))

9

10

11

1

2   **Figure 3b** ((the reflection spectra of the nanocomposite in dry and wet (completely water

3   soaked) states (Ref and λ represent reflection and wavelength, respectively)))
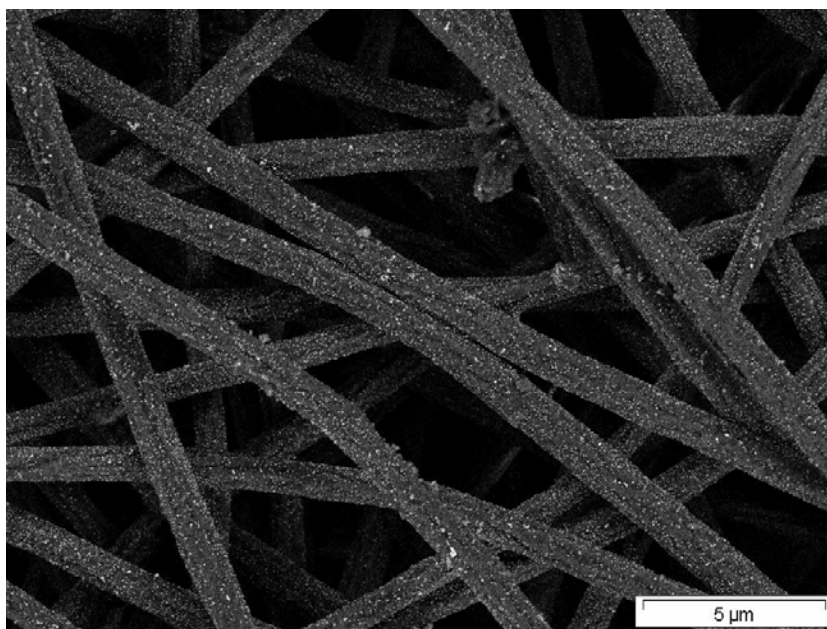
4

5

6

7

8

9

10

11

12

13   **Figure 3c** ((Formation of a bionanohybrid structure through adsorption of Au nanoparticles onto

14   the BSA/PANGMA nanofibers))

15

16

17

1

2

3

4

5

6

7

8

9

S4800 3.0kV 18.0mm x7.00k SE(L)   5.00um

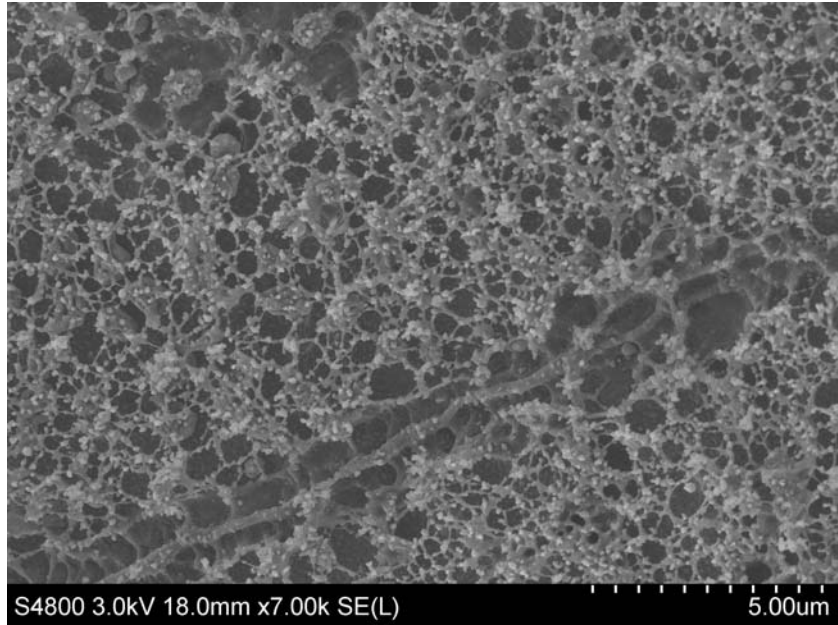10   **Figure 3d** ((Cryo-SEM micrograph showing the surface of the wetted (water soaked)

11   membrane))
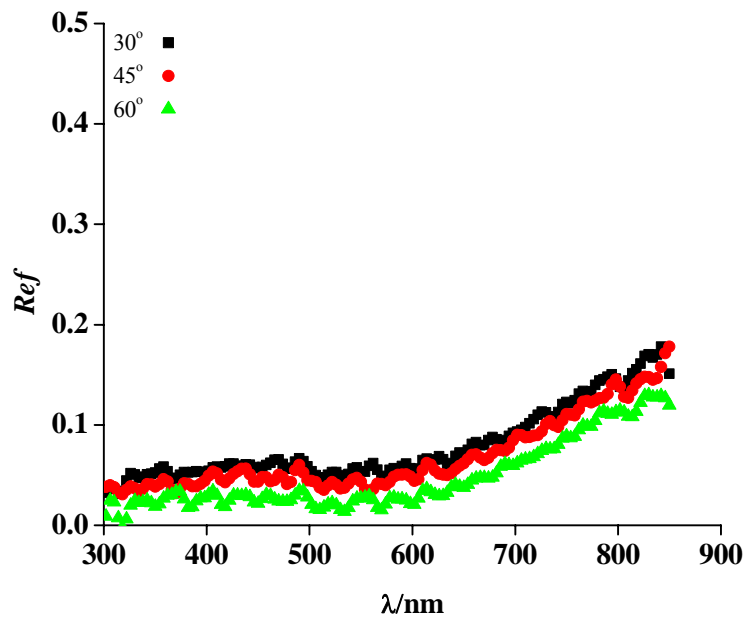

12

13   **Figure 3e** ((the reflection spectra of the black absorber nanocomposite measured at

14   different light incidence angles))
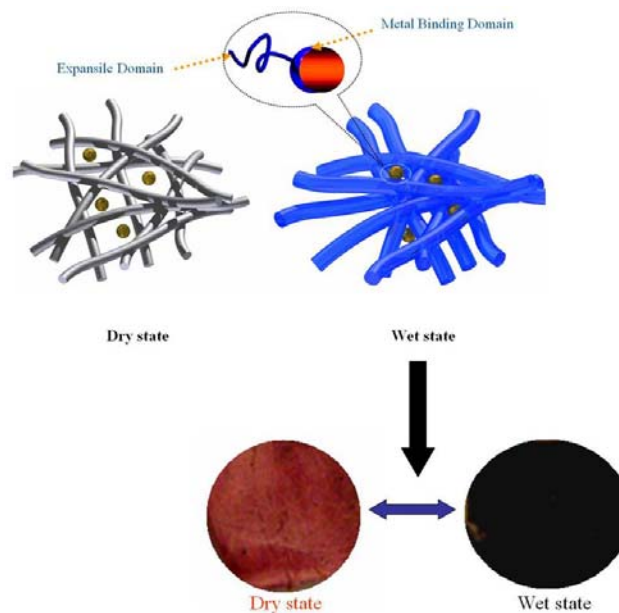
15

1 **The Table of Contents Entry**

2 A smart plasmonic absorber is developed based on a metal-polymer bionanocomposite. A novel

3 fabrication approach is adopted as filtration of a metal nanoparticle containing aqueous suspension by a

4 bio(protein)functionalized nanofibrous membrane. Desirably, nearly all the metal nanoparticles are

5 captured by the protein ligands immobilized onto the nanofibers creating a metal-polymer

6 bionanocomposite. Conformational changes of the protein upon wetting leads to a performance as an

7 omnidirectional black absorber.

8 Keywords: ((plasmonic, black absorber, nanofluid, filtration, bionanocomposite, nanofiber))

9

10 Mady Elbahri[*], Shahin Homaeigohar, Ramzy Abdelaziz, Tianhe Dai, Rania Khalil , Ahnaf Usman

11 Zillohu

12 **Smart Metal-Polymer Bionanocomposites as Omnidirectional Plasmonic Black Absorbers**

13 **Formed by Nanofluid Filtration**

14